Journal of Pharmaceutical and Biomedical Analysis 50 (2009) 27–34

Contents lists available at ScienceDirect

Journal of Pharmaceutical and Biomedical Analysis

journal homepage: www.elsevier.com/locate/jpba

Characterization of metabolic profile of mosapride citrate in rat and identification of two new metabolites: Mosapride *N*-oxide and morpholine ring-opened mosapride by UPLC–ESI-MS/MS

Xiaohong Sun, Lili Niu, Xiaoqin Li, Xiumei Lu, Famei Li *

Department of Analytical Chemistry, Shenyang Pharmaceutical University, Wenhua Road #103, Shenyang 110016, PR China

ARTICLE INFO

Article history:
Received 27 November 2008
Received in revised form 8 March 2009
Accepted 10 March 2009
Available online 24 March 2009

Keywords:
Mosapride
Metabolism
UPLC–ESI-MS/MS
Mosapride *N*-oxide
Morpholine ring-opened mosapride

ABSTRACT

The identification and structure elucidation of metabolites of mosapride, a selective gastroprokinetic agent, was investigated in rats. After oral administration, samples of rat urine, bile, feces and plasma were collected and analyzed by a selective UPLC–ESI-MS/MS method. Altogether 18 metabolites were detected and at least 15 metabolites were reported in rat for the first time. Two new metabolites, mosapride *N*-oxide in rat bile, urine and plasma, morpholine ring-opened mosapride in plasma and feces, were identified by comparison with the reference standards. One known major mammalian metabolite, des-*p*-fluorobenzyl mosapride, was also identified. The molecular structures of nine phase I metabolites and six phase II metabolites of mosapride were elucidated based on the characteristics of their protonated molecular ions, product ions and chromatographic retention times. The phase I metabolites were mainly transformed by four main metabolism pathways, dealkylation, *N*-oxidation, morpholine ring cleavage and hydroxylation, with dealkylation as the predominant metabolic pathway, while phase II metabolites were mainly formed by glucuronidation. The relatively comprehensive metabolic pathway of mosapride was proposed.

1. Introduction

Metabolism studies play an important role in drug discovery and development process. In the past, metabolite identification occurred usually only after a drug candidate had been chosen for drug development. However, drug metabolism can influence a drug's distribution, rate or route of excretion and production of new and possibly active or toxic species. Currently, data on metabolism are used to optimize drug candidates, namely to suggest more active compounds or support further toxicology studies [1–3]. Due to its selectivity, sensitivity and speed of analysis, LC coupled with tandem mass spectrometry (LC–MS/MS) has become an indispensable tool that is needed for all phases of the fast-paced drug discovery and development, especially for metabolite detection and identification even at trace levels in complex matrixes [2,4,5].

Mosapride citrate (mosapride), 4-amino-5-chloro-2-ethoxy-*N*-[[4-(4-fluorobenzyl)-2-morpholinyl]methyl]benzamide citrate, is a potent gastroprokinetic agent that enhances the gastrointestinal (GI) motility and gastric emptying by accelerating acetylcholine release in the GI tract [6]. It is a selective serotonin 5-HT_4 receptor agonist with no affinity for dopamine D_2 receptor [7]. Mosapride has been reported to improve GI symptoms in patients with gastroesophageal reflux disease and to ameliorate constipation and response fluctuations in Parkinsonian patients [8,9]. Due to little arrhythmic effect associated with the QT prolongation, mosapride has been used increasingly in Japan and some other Asian countries [6].

Compared with the comprehensive investigations on its pharmacological activities and therapeutic practices [6,10–14], the study on the metabolism of mosapride in vivo is limited [15–17]. The reported method used for mosapride metabolism was radioisotope labeling-TLC assay. Although it was sensitive, the selectivity of the method was poor and it could not give any information on metabolite structures. Only four metabolites were isolated from rat urine and identified as des-*p*-fluorobenzyl mosapride, 5′-oxo-des-*p*-fluorobenzyl mosapride, 3-hydroxy des-*p*-fluorobenzyl and 3-hydroxy 5′-oxo-des-*p*-fluorobenzyl mosapride [16]. It was reported there were still other metabolites detected but not identified or characterized in rats [15–17]. Some metabolites, such as the polar metabolite(s) in male rat bile, accounted for larger proportion [16]. However, there is no study on the overall metabolic profile of mosapride in vivo.

Therefore, this paper presents the method of ultra performance liquid chromatography (UPLC) coupled with tandem mass

* Corresponding author at: P.O. Box 39, Department of Analytical Chemistry, Shenyang Pharmaceutical University, Wenhua Road #103, Shenyang 110016, PR China. Tel.: +86 24 23986289; fax: +86 24 23986289.
E-mail address: lifamei@syphu.edu.cn (F. Li).

0731-7085/$ – see front matter © 2009 Elsevier B.V. All rights reserved.
doi:10.1016/j.jpba.2009.03.011

spectrometric detection (UPLC–MS/MS) for the characterization of metabolic profile of mosapride in rats. Previously in our group, fungal biotransformation of mosapride by *Cunninghamella* (*C.*) *elegans* AS 3.156 was carried out. Two new compounds, mosapride *N*-oxide and morpholine ring-opened mosapride were produced by putative biotransformation [18]. They were used as reference standards for metabolism study of mosapride in vivo in this paper. The structures of nine phase I metabolites and six phase II metabolites of mosapride were elucidated based on the characteristics of their protonated molecular ions, product ions and chromatographic retention times. The analysis time was only 15 min per run. This approach was found to be essential and superior for the study of mosapride metabolism. The possible metabolic pathways of mosapride were proposed for the first time.

2. Experimental

2.1. Chemical and reagents

Mosapride citrate (Fig. 1), was purchased from Kangning Pharmaceutical Co. (Sanmen County, China). Des-*p*-fluorobenzyl mosapride, mosapride *N*-oxide and morpholine ring-opened mosapride were isolated and purified from the preparative-scale microbial transformation of mosapride and identified as pure compounds by UV, MS, NMR with the purity above 98% by our laboratory [18]. Methanol, acetonitrile and formic acid were of HPLC grade and purchased from Dikma (Richmond Hill, USA). All other chemicals were of analytical grade.

2.2. Animals and drug administration

Male Sprague–Dawley rats (260–350 g, Experimental Animal Research Center of Shenyang Pharmaceutical University, China) were maintained at ambient temperature (22–24 °C) with a 72 h light/dark cycle. All protocols of animal experiments were approved in accordance with the Regulations of Experimental Animal Administration issued by the State Committee of Science and Technology of People's Republic of China. The rats were fasted overnight but with free access to water before use. Mosapride citrate was dissolved in 0.5% carboxymethyl cellulose (CMC) and administered by oral gavage at a dose of 14.5 mg/kg body weight, corresponding to 10 mg/kg body weight of mosapride. CMC at a concentration of 0.5% was administered orally to the rats for blank urine, feces, bile and plasma collections.

2.3. Collection and storage of samples

Blood samples (1 ml) via the orbital sinus were collected into heparinized tubes immediately before (for blank blood sample) and at 0.5, 1, 3, 7 and 12.5 h after oral administration to three rats, respectively. Plasma was harvested by centrifugation at 2000 × *g* for 10 min and stored at −20 °C until analysis.

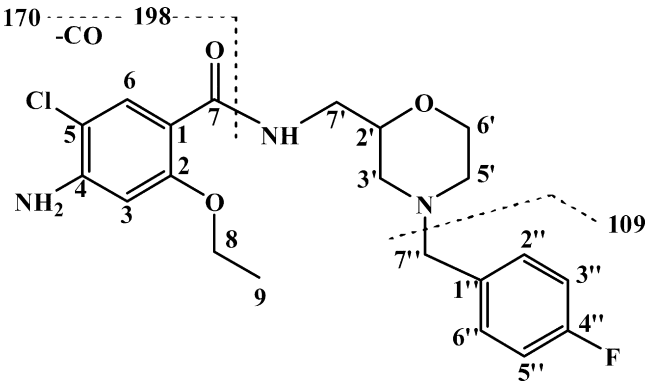

Fig. 1. Structure of mosapride with numbering system and its major ESI(+)-MS/MS fragmentation patterns.

For urine and feces sampling, six rats were divided into two groups and then individually housed in metabolic cages with free access to deionized water. One group consisting of four rats was administered with mosapride and the other was administered with 0.5% CMC for blank sample collection. The excreta were collected into containers surrounded by ice over 0–12, 12–24, 24–36, 36–48 and 48–60 h after dose administration. Cage rinses were performed after each collection interval. After centrifugation of urine samples at 2000 × *g* for 10 min, the supernatant and feces samples were stored at −20 °C until additional extraction and analysis.

For bile sampling, six fasted rats were fixed on a wooden plate and anesthetized with ether. An abdominal incision was made and the common bile duct was cannulated with PE-10 tubing (ID = 0.08 cm, Becton Dickinson, USA) for the collection of bile samples, and closed by suturation. When recovered conscious, four rats were administered with mosapride by oral gavage and the others with 0.5% CMC for blank. A heating lamp was used for maintaining the body temperature during the experimental procedure to prevent hypothermic alterations of the bile flow. Bile samples were collected into containers surrounded by ice during 0–2, 2–4, 4–8, 8–12, 12–24 and 24–36 h periods and stored at −20 °C until additional extraction and analysis.

2.4. Sample preparation

2.4.1. SPE

Oasis MCX® mixed-mode cation-exchange cartridges (1 ml volume, Waters Corp., USA) were conditioned with 1 ml of methanol, 1 ml of water, each twice. Mixed plasma, urine and bile samples were centrifuged at 2000 × *g* for 10 min, the supernatant were removed for use. Urine and bile samples of 0.6 ml were diluted with 0.4 ml of deionized water. Before loaded onto the SPE cartridges, all the samples were filtered through 0.45 μm membrane. Then the SPE cartridges were washed with 1 ml of 1% formic acid aqueous, 1 ml of methanol and eluted with 1 ml of methanol containing 5% ammonium hydroxide. The eluate was evaporated to dryness under a gentle stream of nitrogen at 40 °C, and the residue was dissolved in 200 μl of the mixture of acetonitrile–0.2% formic acid aqueous (3:7, v/v). A small aliquot of 10 μl of the solution was injected into the UPLC–MS/MS system.

2.4.2. Liquid–liquid extraction (LLE)

Feces samples (200 mg) were weighted and supplemented with an appropriate volume (6 ml/g) of the mixture of methanol–water (8:2, v/v). After ultrasonic extraction for 20 min, the samples were centrifuged at 2000 × *g* for 10 min. The supernatant was transferred to a clean tube and 3 ml of ethyl acetate was added. After vortexing and centrifugation at 2000 × *g* for 10 min, the supernatant was transferred to a clean tube and dried under a flow of nitrogen at 35 °C. The residue was reconstituted in 300 μl of methanol. After filtered through 0.45 μm membrane, an aliquot of 10 μl was injected into the UPLC–MS/MS system for analysis.

2.5. Instrumentation and analytical conditions

UPLC–MS/MS system consisted of an ACQUITY™ UPLC system (Milford, MA, USA) and Waters Micromass® Quattro micro™ API mass spectrometer (Manchester, UK) equipped with an ESI source. The chromatographic separation was achieved on an ACQUITY UPLC™ BEH C_{18} column (100 mm × 2.1 mm; ID 1.7 μm; Waters Corp., Milford, MA, USA) with the column temperature set at 40 °C. The flow rate was 0.25 ml/min with a linear gradient running form 84% to 78% A (solvent A, 0.2% formic acid aqueous; solvent B, ace-

tonitrile) in 4 min, 78–76% A in the next 8 min, then to 10% A for 1 min, and returned to initial condition for 2 min for reequilibration. The total run time per sample was 15 min.

As for the MS performed in the positive ESI mode, the optimal MS parameters were as follows: capillary voltage 3.0 kV, cone voltage 30 kV, source temperature 100 °C and desolvation temperature 350 °C. Nitrogen was used as the desolvation and cone gas with a flow rate of 500 and 50 l/h, respectively. For MS/MS analyses, argon was used as the collision gas set at 2.5 e^{-3} mbar, and the collision energy ranged from 18 to 40 eV for all metabolites. Data was acquired and processed using MassLynx™ NT 4.1 software (Waters Corp., Milford, MA, USA).

3. Results and discussion

3.1. Optimization of extraction procedure and analysis conditions

Various sample preparation methods were investigated to select efficient clean-up procedures for biosamples. The methods included LLE with ethyl acetate after alkylation and SPE with Oasis HLB® cartridges (Waters Corp., USA) as well as Oasis MCX® cartridges. For biosamples except feces, LLE and SPE with Oasis HLB® could only extract a few or part of the drug-related compounds and there were high background noises, especially for LLE. In contrast, SPE with Oasis MCX® gave not only more comprehensive targeted drug-related peaks, higher recoveries for mosapride and the metabolites with reference standards, but also less interference from the co-eluted endogenous matrices. For feces samples, LLE and direct ultrasonic extraction with the mixture of methanol–water (8:2, v/v) were investigated and the former was finally chosen considering less interferences and the satisfactory information of metabolites it provided.

To obtain chromatograms with good resolution, acetonitrile–water and methanol–water were investigated and the former was chosen. Various additives of formic acid, acetic acid (both 0.1% and 0.2%, v/v) and ammonium acetate (10 mM) were investigated, and 0.2% (v/v) formic acid gave best separation and peak shape. Therefore, acetonitrile–0.2% formic acid aqueous was chosen as mobile phase for gradient elution. In the present study, the instrumental parameters were optimized by analyzing mosapride standard solution for the maximum intensity. To obtain the most abundant MS/MS information for each of drug-related compounds in rat samples, the collision energy was optimized individually.

3.2. Validation of qualitative assays

The specificity of the assay was evaluated by analyzing blank samples of rats in UPLC–MS/MS mode. No impurity or endogenous interferences were found at the retention time regions of mosapride and its metabolites.

Standard solutions of mosapride, des-*p*-fluorobenzyl mosapride, mosapride *N*-oxide and morpholine ring-opened mosapride at 50 ng/ml were used for the investigation on limit of detection (LoD), recovery, and stability. The LoDs of the above four compounds were 12.5, 10, 25 and 15 ng/ml by UPLC–MS, respectively. The mean recoveries ($n = 3$) ranged from 53.6% to 96.3% with S.D. not more than 5.8% in different biological media (Table 1). Both of the stock solutions (800 μg/ml in methanol) and working solutions (50 ng/ml in methanol–water (1:1, v/v)) were stable for 1 month at −20 °C. The four compounds in blank matrices and the extracted samples were stable for at least 1 month at −20 °C and 48 h at 4 °C, respectively.

In order to investigate the repeatability of area percentage composition of the metabolites in TIC, five replicates from the same urine sample (0–12 h) were prepared and determined. The R.S.D. of repeatability were less than 3.2%.

3.3. Identification and structure elucidation of metabolites

The first step in this work involved the characterization of the mass spectra and LC retention properties of the parent drug. The fragmentation patterns of mosapride served as templates in the elucidation of the structures of the proposed metabolites. The full scan mass spectra and TIC of samples pose-dose were compared with those of the blank and the parent drug to find the potential metabolites, which were then analyzed by UPLC–MS/MS. Identification of metabolites was accomplished by comparison with reference standards, while structure elucidation was facilitated by the fact that the drug-related compounds produce well definable and characteristic product ions under MS/MS conditions. Retention times, changes in observed mass (ΔM) and spectral patterns of product ions of metabolites were compared with those of mosapride to elucidate their structures.

Based on the method mentioned above, 18 metabolites were detected. Two new phase I metabolites (M17 and M18) and 1 known metabolite (M5) were identified with available reference standards prepared in our laboratory, while the structures of other 15 metabolites were elucidated. The parent ion, major product ions and relative abundance of content in biological matrices along with the UPLC retention times of mosapride and its metabolites in rats are summarized in Table 2. UPLC–MS/MS chromatograms of mosapride and its metabolites by daughter scan mode are presented in Fig. 2. Product ion spectra of the protonated molecular ions are presented in Fig. 3.

3.3.1. Mosapride (parent drug)

The compound eluting at 8.17 min had protonated molecular ion $[M+H]^+$ at m/z 422 in the full-scan MS. In the MS/MS spectrum under daughter scan mode, it had typical and most abundant fragment ion at m/z 198 (cleavage at C-7–N), which further lost a neutral moiety of CO to form ion at m/z 170 [18]. The fragment ion at m/z 109 represented the *p*-fluorobenzyl portion formed by *N*-4′-dealkylation (Fig. 1). All the chromatographic and mass spectroscopic properties were identical to those of authentic mosapride. The diagnostic fragment ions at m/z 198 and 170 were characteristic of the benzoyl part, while the one at m/z 109 was characteristic of the *p*-fluorobenzyl part.

3.3.2. Urine metabolites in rats

Metabolite M1, eluted at 1.52 min, had protonated molecular ion $[M+H]^+$ at m/z 506 and fragment ions at m/z 390, 214 and 186 in the MS/MS spectrum. The fragment ions at m/z 214 and 186 were 16 Da higher than those at m/z 198 and 170, which were characteristic ions of mosapride benzoyl moiety. This indicated hydroxylation occurred at C-3 or C-6 position. The fragment ion at m/z 214 was 176 Da lower than that at m/z 390, suggesting a neutral loss of glucuronide. If mosapride has underwent the above two metabolism pathway, the $[M+H]^+$ should be at m/z 614 (614 = 422 + 16 + 176), which is 108 Da higher than that of M1 at m/z 506, this suggests that M1 should be formed by a loss of 4-fluorobenzyl moiety from hydroxyl mosapride glucuronide. Based on the above information, M1 was elucidated as *O*-glucuronide conjugate of des-*p*-fluorobenzyl hydroxymosapride.

Metabolite M2 and M3, eluted at 1.55 and 2.40 min, respectively, showed the same protonated molecular ion $[M+H]^+$ at m/z 330 and fragment ions at m/z 214 and 186, indicating they were isomers formed by hydroxylation at C-3 or C-6 position of benzamide moiety. The molecular ions were 108 Da less than that of hydroxyl mosapride, 438, indicative of a loss of 4-fluorobenzyl moiety. Therefore, M2 and M3 were proposed as des-*p*-fluorobenzyl hydroxymosapride. It was reported 3-hydroxyl des-*p*-fluorobenzyl mosapride was isolated and purified from rat urine after oral administration of mosapride [16]. Due to the lack of reference stan-

Table 1
Recoveries of mosapride and its three metabolites, des-*p*-fluorobenzyl mosapride, mosapride *N*-oxide and morpholine ring-opened mosapride ($n = 3$).

Analytes	Mean recoveries ± S.D. (%)			
	Urine	Bile	Feces	Plasma
Mosapride	84.6 ± 4.4	82.9 ± 3.0	53.6 ± 5.8	89.3 ± 3.2
Des-*p*-fluorobenzyl mosapride	93.4 ± 4.8	88.6 ± 4.1	65.7 ± 4.9	91.5 ± 3.3
Mosapride *N*-oxide	91.7 ± 3.9	96.3 ± 3.5	60.7 ± 5.7	92.4 ± 4.6
Morpholine ring-opened mosapride	90.2 ± 3.7	91.8 ± 3.9	56.3 ± 5.4	86.3 ± 4.0

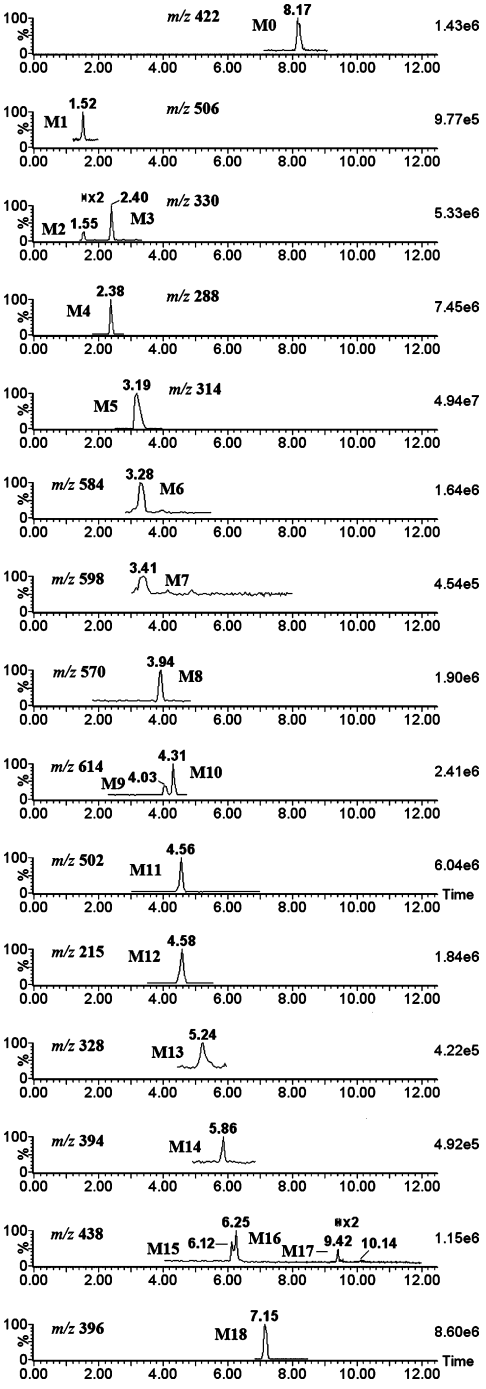

Fig. 2. UPLC–ESI-MS/MS chromatograms of mosapride and its metabolites in rats after oral administration.

dard, we could not define the exact hydroxylation positions of M2 and M3.

Metabolite M4 had a protonated molecular ion $[M+H]^+$ at *m*/*z* 288, with a retention time of 2.38 min. The MS/MS spectra gave prominent ions at *m*/*z* 271, 243, 198 and 170. The presence of fragment ions at *m*/*z* 198 and 170 suggested the unchanged benzoyl part, while the ions at *m*/*z* 271 and 243 were produced by neutral loss of NH_3 and further loss of C_2H_4 via *O*-dealkylation ($243 = 271 - 28$), respectively. Considering the nitrogen rule, we tentatively elucidated M4 to be formed by *N*-dealkylation of 4-fluorobenzyl moiety and cleavage of morpholine ring by neutral loss of C_2H_4.

Metabolite M5, eluted at 3.19 min, showed a protonated molecular ion $[M+H]^+$ at *m*/*z* 314 which is 108 Da less than mosapride and formed by a loss of 4-fluorobenzyl moiety. The corresponding fragment ions at *m*/*z* 198 and 170 were in consistence with the unchanged benzoyl moiety by cleaving at the C-7′–N bond. All of these properties were identical to those of des-*p*-fluorobenzyl mosapride reference standard, so M5 was identified as des-*p*-fluorobenzyl mosapride, which has been reported to be the known major metabolite in experimental animals and humans [16].

Metabolite M7 eluted at 3.41 min had a protonated molecular ion $[M+H]^+$ at *m*/*z* 598, a mass shift of 176 Da compared with the parent mosapride, and fragment ions at *m*/*z* 374, 198 and 170. The fragment ion at *m*/*z* 374 ($374 = 198 + 176$) was the glucuronide conjugated benzoyl moiety and it further produced the ions at *m*/*z* 198 and 170 by losses of glucuronide and CO, respectively. Thus, M7 was proposed as 4-glucuronide-mosapride.

Metabolite M8 was eluted at 3.94 min and gave $[M+H]^+$ at *m*/*z* 570. The MS/MS spectrum produced fragment ions at *m*/*z* 394, 225, 208, 170 and 109. The ion at *m*/*z* 394 was 176 Da less than the protonated molecular ion, indicative of glucuronide conjugation. The fragment ion at *m*/*z* 394 was 28 Da less than that of mosapride and suggested a loss of C_2H_4 via *O*-dealkylation to form 2-phenolic hydroxyl group. It further cleaved at benzamide C–N bond and gave rise to the ions at *m*/*z* 170 and 225, which represented the benzoyl moiety and the rest morpholine ring moiety, respectively. The ion at *m*/*z* 225 further lost a neutral molecular of NH_3 to produce the ion at *m*/*z* 208 ($208 = 225 - 17$). The ion at *m*/*z* 109 was the unchanged 4-fluorobenzyl moiety. Thus, M8 was tentatively assumed to be glucuronide conjugate of *O*-deethyl mosapride

Metabolite M9 and M10, eluted at 4.03 and 4.31 min, respectively, both gave $[M+H]^+$ at *m*/*z* 614, 192 Da more than mosapride, indicating they were isomers formed by addition of an oxygen atom and glucuronidation. The MS/MS spectra produced fragment ions at *m*/*z* 438, 422, 390, 214, 198, 186, 170 for M9 and 390, 214, 186 for M10. The isomers had the same fragment ions formed as follows: 390 was the glucuronide conjugated part of hydroxylated benzamide moiety ($390 = 198 + 16 + 176$), it further produced the ones at *m*/*z* 214 and 186 by neutral losses of glucuronide and CO. Hence, M9 and M10 were assumed to be *O*-glucuronide conjugated of 3-hydroxymosapride or 6-hydroxymosapride. However, the exact phenolic hydroxyl position at C-3 or C-6 could not be fully ascertained from these data.

Metabolite M11 was eluted at 4.56 min and had a protonated molecular ion $[M+H]^+$ at *m*/*z* 502 and fragment ions at *m*/*z* 422,

278, 225, 198, 170 and 109. The fragment ion at *m*/*z* 422 was formed by a neutral loss of sulfate and suggested sulfate conjugation of mosapride. Resulted from cleavage of benzamide C–N bond, the fragment ions at *m*/*z* 278 (278 = 198 + 80) and 225 were the sulfate conjugated benzoyl moiety at 4-NH_2 and the rest moiety, respectively. With the confirmation of the characteristic ions of parent mosapride at *m*/*z* 198, 170 and 109, M11 was elucidated as mosapride-4-sulfate.

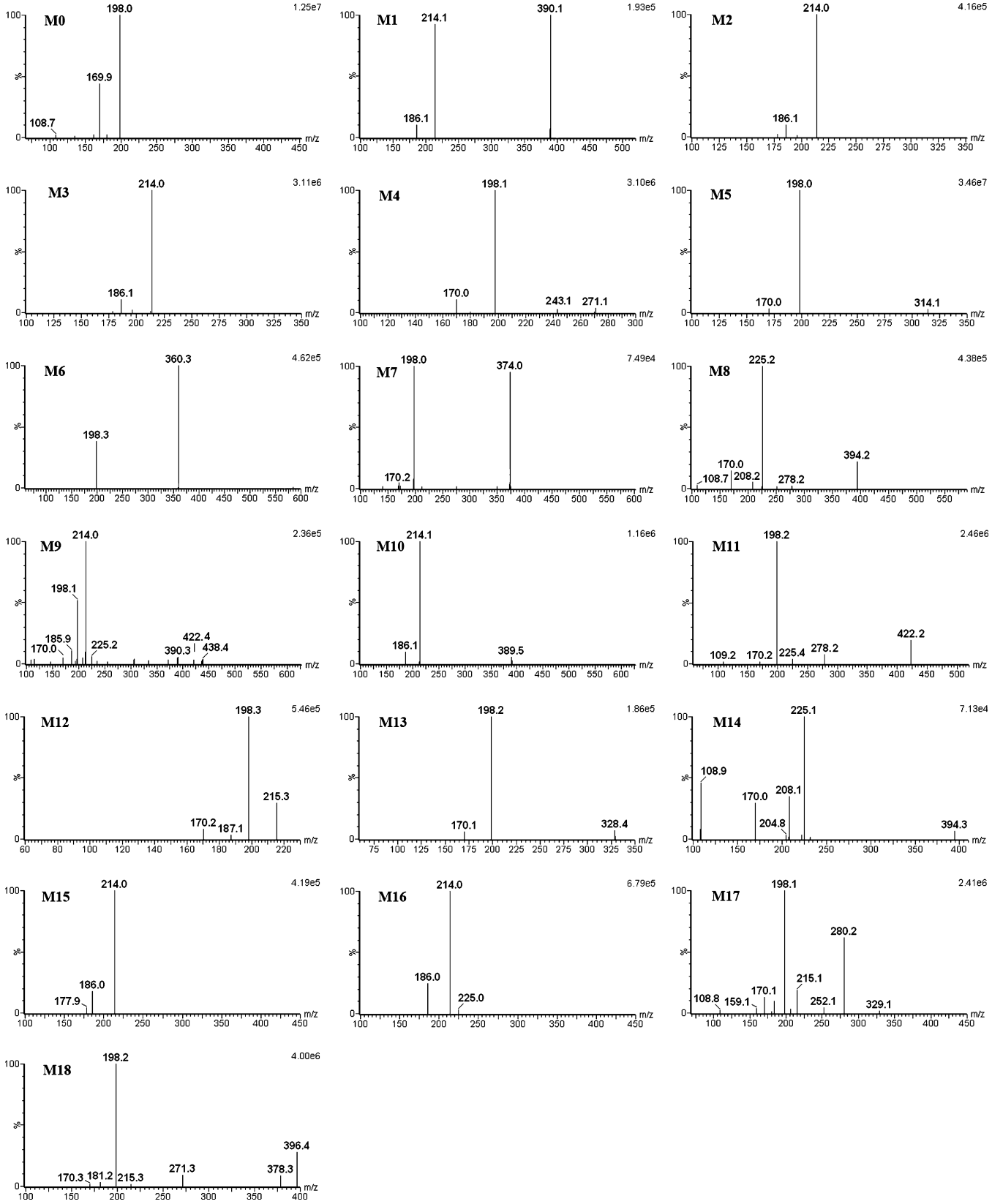

Fig. 3. MS/MS product ion spectra of mosapride and its metabolites in rats.

Table 2
Chromatographic retention times, mass spectrometric data and relative abundance of mosapride and its metabolites in rats after oral administration.

Metabolites	Precursor ion $[M+H]^+$	Retention time (min)	MS/MS data (% base peak)	Urine		Bile		Feces		Plasma	
					Relative abundance (%)		Relative abundance (%)		Relative abundance (%)		Relative abundance (%)
Mosapride	422	8.17	198 (100), 170 (45), 109 (4)	+	1.29	+	55.38	+	74.16	+	38.17
M1	506	1.52	390 (100), 214 (92), 186 (12)	+	18.63	–	–	–	–	–	–
M2	330	1.55	214 (100), 186 (12)	+	0.62	–	–	–	–	–	–
M3	330	2.40	214 (100), 186 (12)	+	4.50	–	–	+	0.37	–	–
M4	288	2.38	271 (5), 243 (4), 198 (100), 170 (12)	+	5.90	–	–	+	0.21	–	–
M5	314	3.19	198 (100), 170 (4)	+	46.58	+	25.85	+	1.77	+	50.89
M6	584	3.28	360 (100), 198 (48)	–	–	–	–	+	0.37	–	–
M7	598	3.41	374 (95), 198 (100), 170 (6)	+	1.09	+	0.64	–	–	–	–
M8	570	3.94	394 (17), 278 (4), 225 (100), 208 (8), 170 (15), 109 (4)	+	9.32	+	0.42	–	–	–	–
M9	614	4.03	438 (4), 422 (4), 390 (8), 225 (8), 214 (100), 198 (53), 186 (12), 170 (6)	+	0.93	+	0.48	–	–	–	–
M10	614	4.31	390 (8), 214 (100), 186 (12)	+	1.86	–	–	–	–	–	–
M11	502	4.56	422 (20), 278 (9), 225 (5), 198 (100), 170 (2), 109 (3)	+	0.78	–	–	+	1.83	–	–
M12	215	4.58	198 (100), 187 (2), 170 (9)	–	–	–	–	+	0.54	–	–
M13	328	5.24	198 (100), 170 (9)	+	1.37	–	–	–	–	+	1.08
M14	394	5.86	225 (100), 208 (29), 170 (27), 109 (47)	+	2.79	–	–	+	10.27	–	–
M15	438	6.12	214 (100), 186 (20)	+	1.24	–	–	+	5.70	+	2.93
M16	438	6.25	214 (100), 186 (40)	+	2.02	–	–	–	–	–	–
M17	438	9.42	329 (2), 280 (60), 252 (5), 215 (19), 198 (100), 170 (13), 159 (5), 109 (2)	+	1.09	+	17.23	–	–	+	5.73
M18	396	7.15	378 (9), 271 (10), 215 (2), 198 (100), 181 (4), 170 (2)	–	–	–	–	+	4.79	+	1.21

(+) found; (–) not found.

M13, eluted at 5.24 min, gave $[M+H]^+$ at *m/z* 328 and fragment ions at *m/z* 198 and 170 in MS/MS spectrum, which indicated unchanged benzoyl moiety. Its molecular weight was 14 Da more than that of M5 (313), suggesting the formation of ketone next to the N atom of morpholine ring according to the drug metabolism rules. It was reported that 5′-oxo-des-*p*-fluorobenzyl mosapride was isolated from rat urine after oral administration of mosapride [16]. Due to lack of reference standard in our laboratory, however, M13 could only be presumed to be 5′-oxo-des-*p*-fluorobenzyl mosapride or 3′-oxo-des-*p*-fluorobenzyl mosapride.

Metabolite M14 was eluted at 5.86 min and had a protonated molecular ion $[M+H]^+$ at *m/z* 394, which was 28 Da less than that of mosapride and indicated a loss of C_2H_4 via *O*-dealkylation to form 2-phenolic hydroxyl group. The MS/MS spectrum gave prominent ions at *m/z* 225, 208, 170 and 109. The ions at *m/z* 170 and 225 were the benzoyl moiety (C_2H_4 less than that of parent mosapride, 170 = 198 – 28) and the rest morpholine ring moiety, respectively, formed via cleavage of benzamide C–N bond. The latter further lost a neutral molecular of NH_3 to produce the ion at *m/z* 208 (208 = 225 – 17). The ion at *m/z* 109 was the unchanged 4-fluorobenzyl moiety. According to the above analyses, M14 was elucidated as *O*-deethyl mosapride.

Metabolites M15, M16 and M17, with retention times of 6.12, 6.25 and 9.42 min, respectively, had the same protonated molecular ions $[M+H]^+$ at *m/z* 438 in the full-scan MS, but had different MS/MS fragment ions, indicating they were isomers. Their 16 Da mass shift from mosapride suggested they were *N*-oxidation or mono-hydroxylation metabolites of mosapride.

The MS/MS spectra of M15 and M16 showed fragment ions at *m/z* 214, 186 and 109, which were in consistent with the hydroxylated benzoyl moiety (214 = 198 + 16, 186 = 170 + 16) and the unaltered 4-fluorobenzyl moiety, respectively. Hence, M15 and M16 were assumed to be 3-hydroxymosapride or 6-hydroxymosapride.

M17 gave fragment ions at *m/z* 329, 280, 252, 215, 198, 170, 159 and 109 in MS/MS. The presence of fragment ions at *m/z* 198, 170 and 109 suggests the addition of O was neither in the benzoyl moiety nor in the 4-fluorobenzyl moiety. The ion at *m/z* 329 resulted from a loss of 4-fluorobenzyl moiety, and it further produced the one at *m/z* 159 by cleavage at the C-1 and C-7 bond. Confirmed by the comparison with reference standard, M17 was identified as mosapride *N*-oxide.

3.3.3. Biliary metabolites in rats

In BDC rat bile, except parent mosapride, two phase I metabolites (M5 and M17) were identified and three phase II glucuronide metabolites (M7–M9) were detected with their structures elucidated.

3.3.4. Feces metabolites in rats

In rat feces, nine metabolites were observed. M3–M5, M11, M14 and M15 were found in rat feces as well as in rat urine, while M6, M12 and M18 were only found in rat feces.

Metabolite M6, eluted at 3.28 min, had a protonated molecular ion $[M+H]^+$ at *m/z* 584 and fragment ions at *m/z* 360 and 198. The protonated molecular ion $[M+H]^+$ was a mass shift of 162 Da compared with the parent mosapride, indicative of glucoside conjugation. The fragment ion at *m/z* 360 (360 = 198 + 162) was the glucoside conjugated benzoyl moiety formed by cleavage at the C-7–N bond. All of these data were consistent with glucoside conjugate of mosapride at 4-NH_2. Thus, M9 was tentatively characterized as 4-glucoside-mosapride.

Metabolite M12, eluted at 4.58 min, gave $[M+H]^+$ at *m/z* 215 and fragment ions at *m/z* 198, 187 and 170. All of the information allowed to postulating on a loss of NH_3 to produce fragment ion at *m/z* 198, which further lost a molecular of CO to form the one at *m/z* 170. The ion at *m/z* 187 was produced by a loss of C_2H_4 from

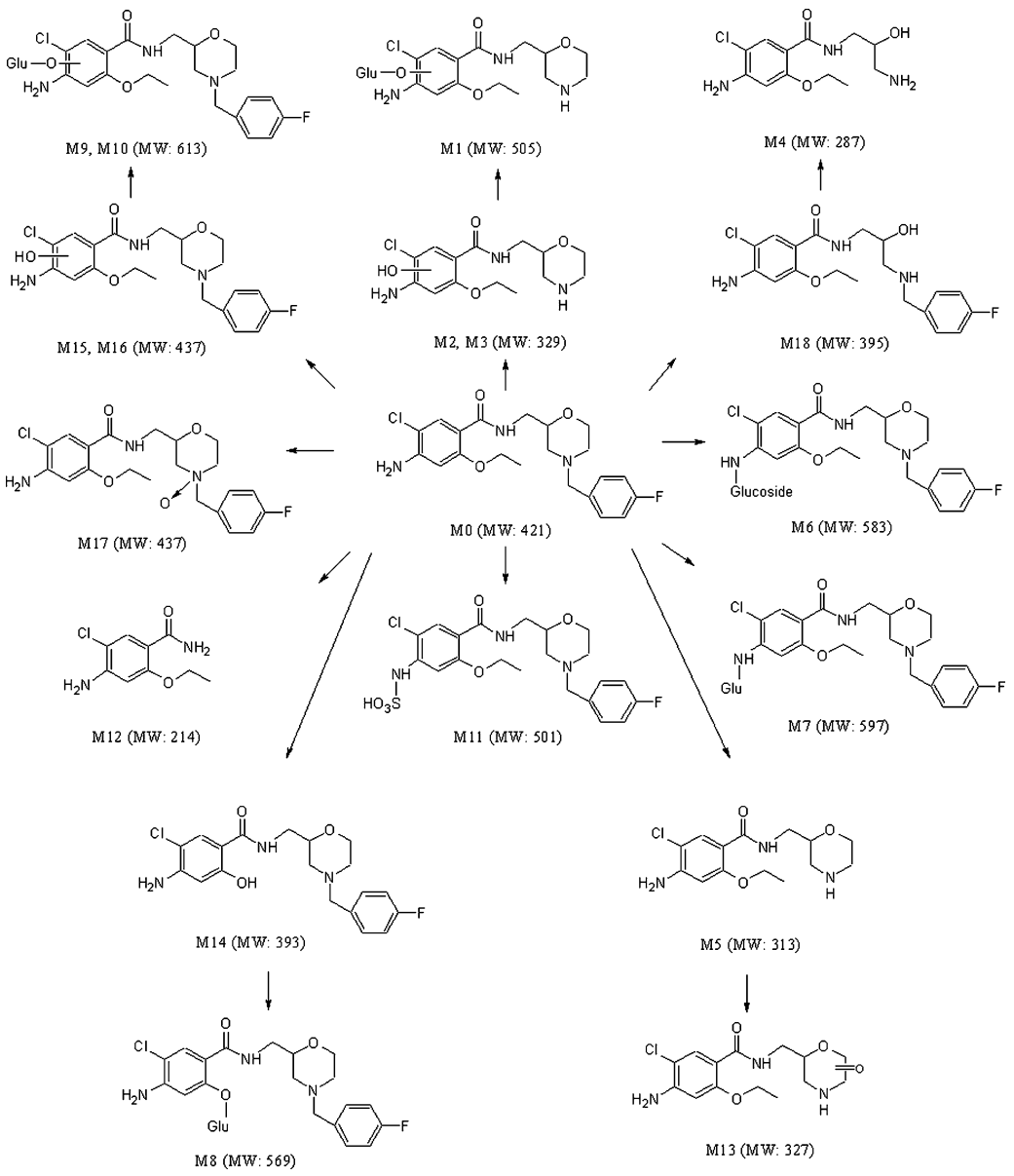

Fig. 4. Proposed metabolic profile of mosapride in rats.

the protonated molecular ion. Therefore, M12 was proposed to be 4-amino-5-chloro-2-ethoxybenzamide.

Metabolite M18 was eluted at 7.15 min and gave $[M+H]^+$ at *m*/*z* 396, which was 26 Da lower than that of mosapride. In MS/MS spectrum, there were fragment ions at *m*/*z* 378, 271, 215, 198, 181 and 170. The presence of *m*/*z* 198 and 170 suggested the unaltered benzoyl moiety, while the ion at *m*/*z* 378 was produced by a loss of water which indicated aliphatic hydroxylation. Thus, we assumed M16 to be the morpholinyl ring-opened metabolite produced by a loss of C_2H_4 (395 = 421 − 28 + 2H) from the morpholinyl ring. The diagnostic ion at *m*/*z* 271 was the benzamide side formed by cleaving at C-3′–NH bond. The fragment ion at *m*/*z* 181 was the 4-fluorobenzyl side formed by cleavage of C-7–NH bond along with a loss of water. M18 was finally identified as morpholine ring-opened mosapride by comparison with the reference standard.

3.3.5. Plasma metabolites in rat

In rat plasma, in addition to parent mosapride, five phase I metabolites, M5, M13, M15, M17 and M18, were detected.

3.4. Elucidation of the possible metabolic pathway

After oral administration of mosapride to rats, a part of absorbed mosapride was well excreted into bile as M5, M17 and three glucuronide metabolites in rats. Subsequently, mosapride and its biliary metabolites were brought into contact with bacterial flora in the intestinal tract. Finally, nine degraded metabolites were excreted from the body into rat feces with mosapride. As could been seen from the structures that M8 in rat bile was the *O*-glucuronide conjugates of M14 in feces and M9 in bile might be the *O*-glucuronide conjugates of M15 in feces. M17 was not detected in rat feces. The striking differences in metabolic profile between the bile and fecal might be explained by the reduction of *N*-oxide metabolites and hydrolysis of the conjugative metabolites during their passage through the GI tract before excretion in the feces. Reduction and hydrolysis by the GI gut flora have been reported for a number of *N*-oxide and conjugative metabolites, respectively [19–21]. The differences in the bile and fecal profiles of mosapride exemplify the utility of BDC animal studies in understanding the

complete metabolism and excretion profile of a drug. Without BDC study, it may be erroneously concluded that the presence of mosapride in feces was caused by incomplete absorption or direct excretion of the parent compound into the bile [21]. The proposed metabolic pathway of mosapride in rats is shown in Fig. 4.

Previously, microbial transformation of mosapride by the filamentous fungus *C. elegans* AS 3.156 was studied by our group with M5, M17 and M18 isolated, purified and identified as pure compounds [18]. These compounds were used as reference standards in this work. Another four metabolites, M6, M11, M12 and M16 were also found in the in vitro microbial transformation system. The results obtained served well as an example of microbial transformation being an in vitro model for mammalian drug metabolism. However, there were obvious differences in metabolic profile between rats and the microbial transformation system: (1) five phase II glucuronide conjugates (M1, M7–M10) were found in rats, while none was found in the microbial system; (2) three phase II metabolites, two formylated and one acetylated metabolites were found in the microbial system [18], while none in rats.

Both in rats and the in vitro microbial system, the metabolism of mosapride has been shown to proceed via *N*-dealkylation and *N*-oxidation occurring at the *N*-heteroatom of morpholine ring. Metabolism of xenobiotics that contain an aliphatic tertiary amine group may result in the formation of *N*-dealkylated and/or *N*-oxygenated products [21–23]. The relative occurrences of these two transformations have been analyzed using structure–activity relationships [24]. The *N*-oxides are frequently reduced back to the parent tertiary amines. The interconversion between tertiary amines and *N*-oxides is a well-known metabolic pathway [25–27]. Such interconversion in the body might be effective to maintain the pharmacological effect of amines and in several cases *N*-oxides are more active than their corresponding tertiary amines. Several *N*-oxides are important as pharmacological or toxicological agents [25]. The interconversion between mosapride and its *N*-oxide metabolite needs further study to fully illustrate the pharmacological effect.

4. Conclusions

The metabolic profile of mosapride in rats was characterized by UPLC–ESI-MS/MS. Three metabolites including two new ones were identified by comparison with corresponding reference standards and the other 15 were elucidated. At least 15 metabolites were reported for the first time in vivo. The phase I metabolites were mainly transformed by four main metabolism routes, dealkylation, *N*-oxidation, morpholine ring cleavage and hydroxylation, with dealkylation as the predominant metabolic pathway. The phase II metabolites were mainly formed by glucuronidation. The possible metabolic pathway of mosapride in vivo was proposed for the first time. This investigation was helpful to better understand the complete in vivo metabolism and excretion of mosapride, which is essential for fully understanding its safety and efficacy.

References

[1] E.J. Oliveira, D.G. Watson, Biomed. Chromatogr. 14 (2000) 351–372.
[2] A.E.F. Nassar, R.E. Talaat, A.M. Kamel, Curr. Opin. Drug Discov. Dev. 9 (2006) 61–74.
[3] N.J. Clarke, D. Rindgen, W.A. Korfmacher, K.A. Cox, Anal. Chem. 73 (2001) 430A–439A.
[4] W.A. Korfmacher, Curr. Drug Metab. 7 (2006) 455–1455.
[5] S. Pedraglio, M.G. Rozio, P. Misiano, V. Reali, G. Dondio, C. Bigogno, J. Pharm. Biomed. Anal. 44 (2007) 665–673.
[6] M.P. Curran, D.M. Robinson, Drugs 68 (2008) 981–991.
[7] N. Yoshida, Nippon Yakurigaku Zasshi 113 (1999) 299–307.
[8] Z. Liu, R. Sakakibara, T. Odaka, T. Uchiyama, T. Uchiyama, T. Yamamoto, T. Ito, M. Asahina, K. Yamaguchi, T. Yamaguchi, T. Hattori, Mov. Disord. 20 (2005) 680–686.
[9] H. Asai, F. Udaka, M. Hirano, T. Minami, M. Oda, T. Kubori, K. Nishinaka, M. Kameyama, S. Ueno, Parkinsonism Relat. Disord. 11 (2005) 499–502.
[10] R. Tomita, S. Igarashi, S. Fujisaki, T. Kusafuka, Hepatogastroenterology 55 (2008) 760–765.
[11] H.S. Kim, E.J. Choi, H. Park, Neurogastroenterol. Motil. 20 (2008) 169–176.
[12] M. He, T. Ohrui, T. Ebihara, S. Ebihara, H. Sasaki, H. Arai, Pneumonia Prevention Study Group, J. Am. Geriatr. Soc. 55 (2007) 142–144.
[13] A. Asakawa, N. Ueno, M. Katagi, Y. Ijuin, Y. Morita, S. Mizuno, T. Inui, R. Sakamaki, N. Shinfuku, M. Uemoto, J. Diab. Complicat. 20 (2006) 56–58.
[14] H. Asakawa, I. Hayashi, T. Fukui, K. Tokunaga, Diab. Res. Clin. Pract. 61 (2003) 175–182.
[15] S. Matsumoto, M. Tagawa, T. Hatoyama, T. Fujii, H. Miyazaki, Y. Sekine, Arzneimittelforschung 43 (1993) 1103–1108.
[16] S. Matsumoto, K. Yoshida, A. Itogawa, M. Tagawa, T. Fujii, H. Miyazaki, Y. Sekine, Arzneimittelforschung 43 (1993) 1095–1102.
[17] M. Sakashita, T. Yamaguchi, H. Miyazaki, Y. Sekine, T. Nomiyama, S. Tanaka, T. Miwa, S. Harasawa, Arzneimittelforschung 43 (1993) 867–872.
[18] X.H. Sun, F. Man, L.Y. Pang, G.H. Gao, X.Q. Li, X.L. Qi, F.M. Li, Fungal biotransformation of mosapride by *Cunninghamella elegans*, doi:10.1016/j.molcatb.2009.01.009.
[19] R.J. Parker, P.C. Hirom, P. Millburn, Xenobiotica 10 (1980) 689–703.
[20] S.C. Mitchell, A.Q. Zhang, J.M.D. Noblet, S. Gillespie, N. Jones, R.L. Smith, Xenobiotica 27 (1997) 1187–1197.
[21] L.J. Christopher, D.H. Cui, W.Y. Li, A. Barros, V.K. Arora, H.Y. Zhang, L.F. Wang, D.L. Zhang, J.A. Manning, K. He, A.M. Fletcher, M. Ogan, M. Lago, S.J. Bonacorsi, W.G. Humphreys, R.A. Iyer, Drug Metab. Dispos. 36 (2008) 1341–1356.
[22] M.C. Dumasia, P. Teale, J. Pharm. Biomed. Anal. 36 (2005) 1085–1091.
[23] H. Chen, Y. Chen, P. Du, F. Han, H. Wang, H. Zhang, J. Pharm. Biomed. Anal. 40 (2006) 142–150.
[24] E.M. Gifford, Structure–reactivity maps as a tool for visualizing xenobiotic structure–reactivity relationships, http://www.netsci.org/Science/Special/feature04.html.
[25] M.H. Bickel, Pharmacol. Rev. 21 (1969) 325–355.
[26] M. Ruth, B. Hamelin, L. Lundell, K. Rohss, Gastroenterology 110 (1996) A245–A1245.
[27] A. Kousba, R. Soll, S. Yee, M. Martin, Drug Metab. Dispos. 35 (2007) 2242–2251.